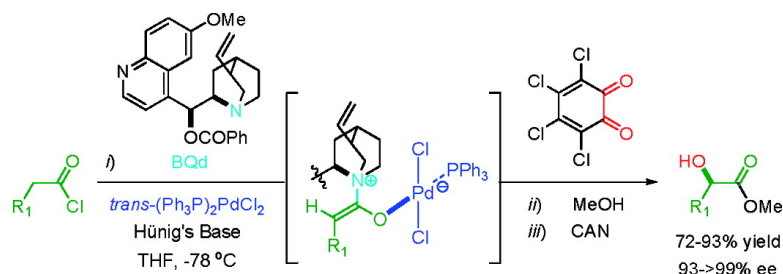


## A Surprising Mechanistic “Switch” in Lewis Acid Activation: A Bifunctional, Asymmetric Approach to $\beta$ -Hydroxy Acid Derivatives

Ciby J. Abraham, Daniel H. Paull, Tefsit Bekele, Michael T. Scerba, Travis Dudding, and Thomas Lectka

*J. Am. Chem. Soc.*, **2008**, 130 (50), 17085-17094 • DOI: 10.1021/ja806818a • Publication Date (Web): 17 November 2008

Downloaded from <http://pubs.acs.org> on February 8, 2009



### More About This Article

Additional resources and features associated with this article are available within the HTML version:

- Supporting Information
- Access to high resolution figures
- Links to articles and content related to this article
- Copyright permission to reproduce figures and/or text from this article

[View the Full Text HTML](#)

## A Surprising Mechanistic “Switch” in Lewis Acid Activation: A Bifunctional, Asymmetric Approach to $\alpha$ -Hydroxy Acid Derivatives

Ciby J. Abraham,<sup>†</sup> Daniel H. Paull,<sup>†</sup> Tefsit Bekele,<sup>†,§</sup> Michael T. Scerba,<sup>†</sup> Travis Dudding,<sup>‡</sup> and Thomas Lectka<sup>\*,†</sup>

Department of Chemistry, New Chemistry Building, Johns Hopkins University, 3400 North Charles Street, Baltimore, Maryland 21218, and Department of Chemistry, Brock University, St. Catharines, Ontario L2S 3A1, Canada

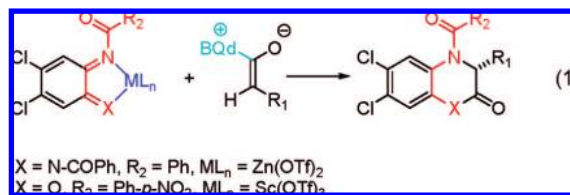
Received August 29, 2008; E-mail: lectka@jhu.edu

**Abstract:** We report a detailed synthetic and mechanistic study of an unusual bifunctional, sequential hetero-Diels–Alder/ring-opening reaction in which chiral, metal complexed ketene enolates react with *o*-quinones to afford highly enantioenriched,  $\alpha$ -hydroxylated carbonyl derivatives in excellent yield. A number of Lewis acids were screened in tandem with cinchona alkaloid derivatives; surprisingly, *trans*-(Ph<sub>3</sub>P)<sub>2</sub>PdCl<sub>2</sub> was found to afford the most dramatic increase in yield and rate of reaction. A series of Lewis acid binding motifs were explored through molecular modeling, as well as IR, UV, and NMR spectroscopy. Our observations document a fundamental mechanistic “switch”, namely the formation of a tandem Lewis base/Lewis acid activated metal enolate in preference to a metal-coordinated quinone species (as observed in other reactions of *o*-quinone derivatives). This new method was applied to the syntheses of several pharmaceutical targets, each of which was obtained in high yield and enantioselectivity.

### Introduction

Few things are as intriguing to the organic chemist as a reaction that takes an unexpected turn when subjected to subtle changes in conditions, substrates, catalysts, or reagents. Particularly interesting examples arise when a change in catalyst compels a reaction to “switch” its mechanistic pathway in a dramatic fashion. Some time ago we observed that a change in the nature of a simple Lewis acid (from “oxophilic” to “azaphilic”) radically altered the catalyzed ring-opening reactions of *N*-acylaziridines.<sup>1</sup> In more recent work, we have found that nucleophilic, cinchona alkaloid based catalysts work in tandem with Lewis acidic metal salts (based on In<sup>III</sup>, Zn<sup>II</sup>, and Sc<sup>III</sup>) to enhance the highly asymmetric reactions of chiral ketene enolate intermediates with *o*-benzoquinone imides and diimides (eq 1).<sup>2</sup> Preliminary mechanistic studies revealed that the Lewis acid activates the quinone derivative through a classical chelate interaction, thereby enhancing its electrophilicity, a result that was more or less expected.

Building on this success, we reasoned that an analogous bifunctional approach to  $\alpha$ -hydroxy carbonyl derivatives, based on our preliminarily communicated results on the cycloaddition



of *o*-benzoquinones and chiral ketene enolates,<sup>3</sup> was feasible. To our surprise, classical Lewis acid “cocatalysts” do not work to enhance yields in this case (though they can in some cases conspire to diminish the yields), but phosphine complexes from the middle of the transition series (based on Ni<sup>II</sup>, Pd<sup>II</sup>, and Pt<sup>II</sup>) do enhance yields, in some cases dramatically, and afford products in high enantioselectivity as well. We present evidence that the reaction of *o*-quinones undergoes a mechanistic “switch” in which the mode of activation changes from Lewis acid (LA) complexation of the quinone to metal complexation of the chiral ketene enolate (which forms from the reaction of the cinchona alkaloid nucleophile (LB) with a ketene). In this paper, we report the first application of catalytic, tandem LA/LB activated ketene enolates to inverse-electron-demand hetero-Diels–Alder reactions with *o*-benzoquinones. This method relies on the activation of catalytically generated chiral ketene enolates by an achiral Lewis acid, notably *trans*-bistriphenylphosphine palladium(II) chloride, and produces highly optically enriched  $\alpha$ -hydroxylated carbonyl derivatives in excellent yield from commercially available *o*-quinones (Scheme 1). Detailed mechanistic evidence for enolate formation is presented, and the synthetic potential

<sup>†</sup> Johns Hopkins University.

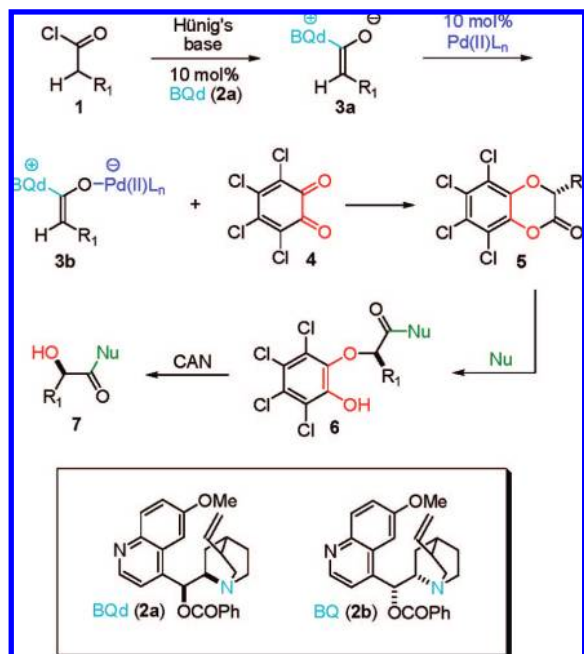
<sup>‡</sup> Brock University.

<sup>§</sup> Present address: A.M.R.I., 26 Corporate Circle, Albany, NY, 12203.

(1) Ferraris, D.; Drury, W. J., III.; Cox, C.; Lectka, T. *J. Org. Chem.* **1998**, *63*, 4568–4569.

(2) (a) Abraham, C. J.; Paull, D. H.; Scerba, M. T.; Grebinski, J. W.; Lectka, T. *J. Am. Chem. Soc.* **2006**, *128*, 13370–13371. (b) Paull, D. H.; Alden-Danforth, E.; Wolfer, J.; Dogo-Isonagie, C.; Abraham, C. J.; Lectka, T. *J. Org. Chem.* **2007**, *72*, 5380–5382. (c) Paull, D. H.; Wolfer, J.; Grebinski, J. W.; Weatherwax, A.; Lectka, T. *Chimia* **2007**, *61*, 240–246. (d) Paull, D. H.; Abraham, C. J.; Scerba, M. T.; Alden-Danforth, E.; Lectka, T. *Acc. Chem. Res.* **2008**, *41*, 655–663.

(3) Bekele, T.; Shah, M. H.; Wolfer, J.; Abraham, C. J.; Weatherwax, A.; Lectka, T. *J. Am. Chem. Soc.* **2006**, *128*, 1810–1811.

**Scheme 1.** Bifunctional Approach to  $\alpha$ -Hydroxylated Carbonyl Derivatives

of this reaction is illustrated in the synthesis of several pharmaceutically and optically active,  $\alpha$ -hydroxylated targets.

## Results and Discussion

In medicinal, biological, and synthetic chemistry alike, chiral  $\alpha$ -hydroxylated carbonyl derivatives play a ubiquitous role; they are found in a diverse array of pharmaceuticals of which recent examples include selective M3 type muscarinic receptor antagonists for the treatment of pulmonary disorders,<sup>4</sup> inhibitors of amyloid- $\beta$  protein,<sup>5</sup>  $\gamma$ -secretase inhibitors for the treatment of Alzheimer's disease,<sup>6</sup> bradykinin B1 antagonists,<sup>7</sup> and a number of antibiotics and anticancer agents.<sup>8</sup> In particular,  $\alpha$ -hydroxyesters, ketones, and amides are present in an astonishing array of natural products<sup>9</sup> and serve as chiral building blocks for the synthesis of complex molecules.<sup>10</sup> They have found use as chiral auxiliaries for enantioselective reactions as well.<sup>11</sup>

The efficient, stereocontrolled production of  $\alpha$ -hydroxycarbonyl compounds has presented an enticing challenge in the field of asymmetric synthesis. Initial methods focused on the

use of chiral auxiliaries,<sup>12</sup> but the need for stoichiometric amounts of chiral materials, in addition to the limitations associated with integration, removal, and recovery of these groups, has led to more practical routes. These include catalytic, asymmetric epoxidation of  $\alpha,\beta$ -unsaturated amides and ketones followed by regioselective epoxide opening,<sup>13</sup> asymmetric reductive coupling of alkynes and aldehydes with subsequent oxidation,<sup>14</sup> phase transfer catalysis,<sup>15</sup> chiral Lewis acid catalysis,<sup>16</sup> kinetic resolution,<sup>17</sup> and enzymatic methods.<sup>18</sup> Other notable examples include a recent enantioselective  $\alpha$ -addition of isocyanides to aldehydes<sup>19</sup> and a rhodium carbenoid-initiated Claisen rearrangement.<sup>20</sup> A mild and practical catalytic, asymmetric approach to their design is necessitated by the increasing number of optically active intermediates and pharmaceuticals containing  $\alpha$ -hydroxylated carbonyl fragments.

While *o*-benzoquinones have received much attention for their roles in redox chemistry,<sup>21</sup> their application in asymmetric synthesis has been largely ignored, though recent work in our laboratory has demonstrated that *o*-quinones can serve as attractive precursors to  $\alpha$ -hydroxy carbonyl derivatives (Scheme 1).<sup>3</sup> In this preliminary work, we reported the first catalytic asymmetric synthesis of  $\alpha$ -oxygenated carbonyl derivatives through a [4 + 2] cycloaddition intermediate using chiral ketene enolates and *o*-quinones. For instance, 10 mol% BQd (**2a**) catalyzed the reaction of *o*-chloranil (**4**) and isovaleryl chloride in the presence of Hünig's base to form cycloadduct **5a** ( $R_1 = i$ -Pr). Methanol was then added, and the aryl group was cleaved with ceric ammonium nitrate (CAN) forming  $\alpha$ -hydroxy ester **7a** in 55% yield and 93% ee. While this method affords  $\alpha$ -hydroxy esters with excellent enantioselectivity, greater efforts were needed to improve the yield.

**A Bifunctional System.** Our catalytic, asymmetric bifunctional system for the alkylation of *o*-benzoquinone diimides by ketene enolates forms products in high yield and in virtual enantiospecificity.<sup>2a</sup> The reaction combines cinchona alkaloid derivatives and  $Zn(OTf)_2$  as cooperative cocatalysts; preliminary evidence is consistent with the most obvious mechanism, namely, catalytic enolate formation by the nucleophilic cinchona alkaloid and simultaneous Lewis acid activation of the metal-chelating diimides (**8**, Figure 1). This putative metal binding was again seen with quinone imides (**9**).<sup>2b</sup>

We began our investigation into a bifunctional system for *o*-quinone alkylation by employing much the same strategy—namely by screening metal cocatalysts that we believed would

- (4) Mase, T.; et al. *J. Org. Chem.* **2001**, *66*, 6775–6786.  
 (5) Wallace, O. B.; Smith, D. W.; Deshpande, M. S.; Polson, C.; Felsenstein, K. M. *Bioorg. Med. Chem. Lett.* **2003**, *13*, 1203–1206.  
 (6) Prasad, C. V. C.; et al.; *Bioorg. Med. Chem. Lett.* **2007**, *17*, 4006–4011.  
 (7) Wood, M. R.; et al.; *Bioorg. Med. Chem. Lett.* **2008**, *18*, 716–720.  
 (8) Guenard, D.; Gueritte-Voegelein, F.; Poiter, P. *Acc. Chem. Res.* **1993**, *26*, 160–167.  
 (9) Recent examples include: (a) Wen, T.; Ding, Y.; Deng, Z.; Ofwegen, L.; Proksch, P.; Lin, W. *J. Nat. Prod.* **2008**, *71*, 1133–1140. (b) Wang, N.; Song, J.; Jang, K. H.; Lee, H.; Li, X.; Oh, K.; Shin, J. *J. Nat. Prod.* **2008**, *71*, 551–557. (c) Ding, G.; Liu, S.; Guo, L.; Zhou, Y.; Che, Y. *J. Nat. Prod.* **2008**, *71*, 615–618. (d) Ishiyama, H.; Okubo, T.; Yasuda, T.; Takahashi, Y.; Iguchi, K.; Kobayashi, J. *J. Nat. Prod.* **2008**, *71*, 633–636. (e) Taori, K.; Matthew, S.; Rocca, J. R.; Paul, V. J.; Leusch, H. *J. Nat. Prod.* **2007**, *70*, 1593–1600.  
 (10) (a) Coppola, G. M.; Schuster, H. F.  *$\alpha$ -Hydroxy Acids in Enantioselective Synthesis*; Wiley-VCH: Weinheim, 1997. (b) Hanessian, S. *Total Synthesis of Natural Products: The Chiron Approach*; Pergamon: New York, 1983.  
 (11) Davies, H. M. L.; Huby, N. J. S.; Cantrell, W. R.; Olive, J. L. *J. Am. Chem. Soc.* **1993**, *115*, 9468–9479.

- (12) (a) Enders, D.; Bhushan, V. *Tetrahedron Lett.* **1988**, *29*, 2437–2440. (b) Davis, F.; Weismiller, M. C. *J. Org. Chem.* **1990**, *55*, 3715–3717. (c) Yu, H. C.; Ballard, E.; Boyle, P. D.; Wang, B. *Tetrahedron* **2002**, *58*, 7663–7679.  
 (13) (a) Kakei, H.; Nemoto, T.; Ohshima, T.; Shibasaki, M. *Angew. Chem., Int. Ed.* **2004**, *43*, 317–320. (b) Nemoto, T.; Kakei, H.; Gnanadesikan, V.; Tosaki, S.; Ohshima, T.; Shibasaki, M. *J. Am. Chem. Soc.* **2002**, *124*, 14544–14545.  
 (14) (a) Cho, C.; Krische, M. J. *Org. Lett.* **2006**, *8*, 891–894. (b) Miller, K. M.; Huang, W.; Jamison, T. F. *J. Am. Chem. Soc.* **2003**, *125*, 3442–3443.  
 (15) Ooi, T.; Fukumoto, K.; Maruoka, K. *Angew. Chem., Int. Ed.* **2006**, *45*, 3839–3842.  
 (16) Christensen, C.; Juhl, K.; Hazell, R.; Jorgensen, K. A. *J. Org. Chem.* **2002**, *67*, 4875–4881.  
 (17) Huerta, F. F.; Santosh Laxmi, Y. R.; Backvall, J. *Org. Lett.* **2000**, *2*, 1037–1040.  
 (18) Zhang, W.; Wang, P. G. *J. Org. Chem.* **2000**, *65*, 4732–4735.  
 (19) Denmark, S. E.; Fan, Y. *J. Org. Chem.* **2005**, *70*, 9667–9676.  
 (20) Wood, J. L.; Moniz, G. A.; Pflum, D. A.; Stoltz, B. M.; Holubec, A. A.; Dietrich, H. *J. Am. Chem. Soc.* **1999**, *121*, 1748–1749.  
 (21) Kharisov, B. I.; Méndez-Rojas, M. A.; Garnovskii, A. D.; Ivakhnenko, E. P.; Ortiz-Méndez, U. *J. Coord. Chem.* **2002**, *55*, 745–770.

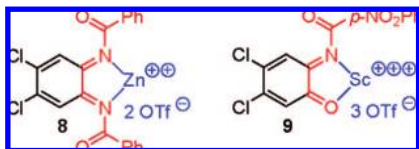


Figure 1. Lewis acid coordination by *o*-benzoquinone derivatives.

Table 1. Lewis Acids Screened under Standard Reaction Conditions

entry	metal (ML <sub>n</sub> )	5 <sup>a</sup> product		7 <sup>a</sup> <sup>b</sup>	
		% ee	% yield	% ee	% yield
1	(Ph <sub>3</sub> P) <sub>2</sub> Pd(SbF <sub>6</sub> ) <sub>2</sub>	--	trace	--	trace
2	(Ph <sub>3</sub> P) <sub>2</sub> CuClO <sub>4</sub>	--	trace	--	trace
3	Sc(OTf) <sub>3</sub>	92	65	92	48
4	Sm(OTf) <sub>3</sub>	90	68	90	50
5	In(OTf) <sub>3</sub>	93	70	93	52
6	Zn(OTf) <sub>2</sub>	92	71	92	53
7	no metal	93	75	93	55
8	PtCl <sub>2</sub>	92	78	92	58
9	PdCl <sub>2</sub>	93	82	93	62
10	(bdppp)NiCl <sub>2</sub>	93	84	93	69
11	(Ph <sub>3</sub> P) <sub>2</sub> NiCl <sub>2</sub> <sup>c</sup>	94	85	94	69
12	<i>cis</i> -(Ph <sub>3</sub> P) <sub>2</sub> PtCl <sub>2</sub>	91	86	91	71
13	<i>trans</i> -(Ph <sub>3</sub> P) <sub>2</sub> PtCl <sub>2</sub>	91	93	91	78
14	(Ph <sub>3</sub> P) <sub>2</sub> PdCl <sub>2</sub> <sup>c</sup>	93	96	93	82
15	<i>trans</i> -(Ph <sub>3</sub> P) <sub>2</sub> PdCl <sub>2</sub>	93	98	93	88

<sup>a</sup> Reactions run with 1 equiv of isovaleryl chloride, chloranil, Hünig's base, and 10 mol% ML<sub>n</sub> and BQd in THF at -78 °C; when completed, worked up by filtering through silica and eluting with hexanes.

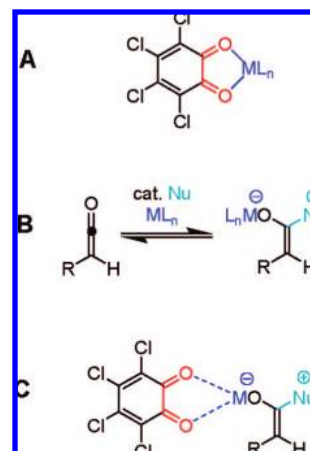
<sup>b</sup> Reactions run as previously mentioned except quenched with MeOH when completed, then solvent replaced with MeCN/H<sub>2</sub>O, and CAN added at -10 °C; product isolated by column chromatography.

<sup>c</sup> Mixture of *cis* and *trans* isomers.

activate the *o*-quinone, especially Lewis acidic and oxophilic metal salts (Table 1). However, we immediately encountered some surprises. Namely, oxophilic metal salts had a marginally detrimental effect on product yields and rates of reaction at best. Although not optimistic of success, we then turned to azaphilic and redox active metals from the middle of the transition series. For example, Cu<sup>I</sup> and Pd<sup>II</sup> complexes with weakly coordinating anions essentially failed, perhaps due to catalyst quenching. On the other hand, when we employed chloride salts of Ni<sup>II</sup>, Pd<sup>II</sup>, and Pt<sup>II</sup>, the yields began to increase substantially. After screening a range of metal complexes (Table 1), we found that *trans*-(Ph<sub>3</sub>P)<sub>2</sub>PdCl<sub>2</sub> gave the highest increase in yield and, therefore, was used in most subsequent reactions. Yields increased by as much as 60% when 10 mol%<sup>22</sup> *trans*-(Ph<sub>3</sub>P)<sub>2</sub>PdCl<sub>2</sub> was employed as our Lewis acid cocatalyst, forming **7a** in 88% yield with full preservation of the high enantioselectivity observed in the metal-free reaction. Thus, we endeavored to reveal how this bifunctional catalytic system,

(22) 10 mol% catalyst was usually employed for screening purposes. While under revision, we observed that significantly lower catalyst loadings (3 mol%) could be employed without significant erosion of ee or yield.

Scheme 2. Possible Binding Scenarios for Cocatalysts



which combines the unlikely cocatalyst pair of a soft, azaphilic Pd<sup>II</sup>-based Lewis acid<sup>23</sup> and a chiral tertiary amine nucleophile, achieves the increase in yields.

**Possible Scenarios.** In our previous bifunctional catalytic studies on Diels–Alder heterodienes (*o*-quinone derivatives), we found that both *o*-benzoquinone imides and diimides were activated by Lewis acids through coordination. Scenario A (Scheme 2) illustrates how a Lewis acid would coordinate to *o*-chloranil if it followed this expected pattern. The second mechanistic possibility is that the Lewis acid is coordinating to the ketene enolate and/or increasing its concentration (B, Scheme 2) and potentially increasing its reactivity. A third possibility is that the Lewis acid is coordinating to both the quinone and ketene enolate in a termolecular complex (C, Scheme 2).

The first scenario was addressed by trying to gather evidence of binding between *o*-chloranil and a Lewis acid. The Pd<sup>II</sup> catalyst and *o*-chloranil were combined under different conditions, varying concentration, solvent, and temperature. IR and <sup>13</sup>C NMR data both routinely failed to show any evidence of binding whatsoever; in fact, IR data for each of the metal salts in Table 1 show no evidence of binding to *o*-chloranil under any conditions attempted. A literature search also fails to provide much evidence for metal complexes of *o*-chloranil, whereas our earlier work showed that Lewis acid binding to more Lewis basic *o*-quinone imides and diimides was favorable, consistent with a classical mechanism. While the absence of observable binding is not compelling evidence by itself (we cannot rule out a small concentration of a highly active LA–LB intermediate), another consideration bolsters our case. The coordinating oxygens of *o*-chloranil should prefer to bind (and be activated by) oxophilic, or “hard” Lewis acids, in Pearson's terminology.<sup>24</sup> Hard Lewis acids, though, are completely ineffective cocatalysts, whereas a “soft” Lewis acid, based on Pd<sup>II</sup>, with a lower presumed affinity for *o*-chloranil, is a highly effective cocatalyst. Consequently, hard–soft LA–LB considerations also argue against a classical Lewis acid activation of *o*-chloranil (see shortly below).

(23) (a) Fowler, J. M.; Griffiths, A. *Acta Crystallogr., Sect. B* **1978**, *34*, 1709–1710. (b) Fowler, J. M.; Griffiths, A. *Acta Crystallogr., Sect. B* **1978**, *34*, 1711–1712. (c) Fowler, J. M.; Griffiths, A. *Acta Crystallogr., Sect. B* **1978**, *34*, 1712–1713.

(24) Pearson, R. G. *J. Am. Chem. Soc.* **1963**, *85*, 3533–3539.



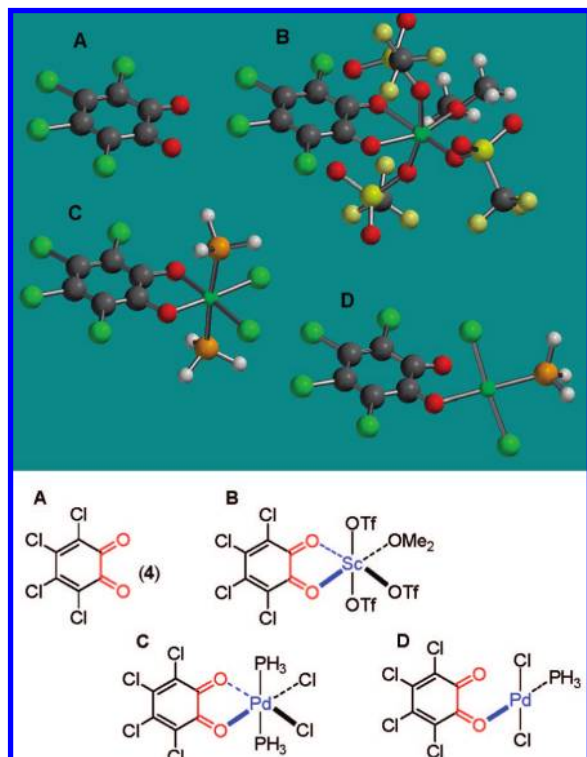
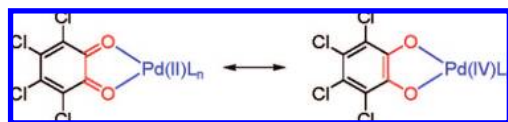


Figure 2. Computational analysis of putative *o*-chloranil–metal complexes.

Scheme 3. Resonance Tautomerization of Putative Pd<sup>(III/IV)</sup>-Bound Quinone: Is Pd<sup>II</sup> a Lewis Base to *o*-Chloranil?



#### Density Functional Theory Calculations for *o*-Chloranil.<sup>25</sup>

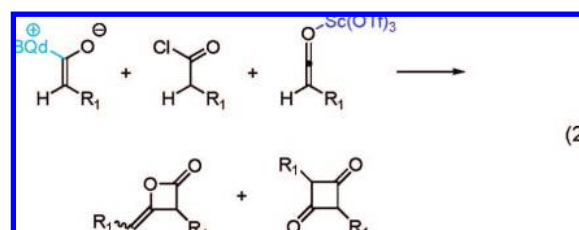
Another interesting clue as to what may be occurring was initially provided by theoretical calculations on putative metal complexes of *o*-chloranil and several Lewis acids (Figure 2). For example, when a *o*-chloranil–Sc(OTf)<sub>3</sub> complex was computed at B3LYP/LANL2DZ, a low energy structure revealed simultaneous coordination to both oxygen atoms, as expected (B, Figure 2). When compared to a control calculation of *o*-chloranil (A, Figure 2), the calculated charge on the ring carbonyl carbon increases,<sup>26</sup> also an expected result for classical Lewis acid activation. However, when the complex *o*-chloranil–*trans*-(Ph<sub>3</sub>P)<sub>2</sub>PdCl<sub>2</sub> was compared (C, Figure 2), the charge on the same carbon decreased, indicating that Pd<sup>II</sup> had transferred electron density into the ring, resembling a complex of Pd<sup>IV</sup> with perchlorocatechol (Scheme 3). In the case of the monodentate square-planar complex D (Figure 2), charges on the carbonyl carbon indicate minor electron donation by the palladium. Because these calculations focus on the carbon charge, where the binding structure is identical in each case,

(25) All calculations were performed using either Spartan 2006, Wavefunction, Inc. (Hartree-Fock) or Gaussian 03: IA32L-G03RevD.01 (Density Functional Theory); see Supporting Information for details.

(26) Partial charge (APT) calculated for the following: (A), bare *o*-chloranil, 0.550; (B), scandium(III) triflate complex of *o*-chloranil, 0.898–0.932; (C), putative (diphosphine)-PdCl<sub>2</sub> complex of *o*-chloranil, 0.383; (D), putative square-planar (monophosphine)-PdCl<sub>2</sub> complex of *o*-chloranil, 0.401–0.442.

they reflect more accurately the electronic influence of the metal on the quinone system. These calculations also suggest that Pd<sup>II</sup> in this case should not be a good Lewis acid activator of the *o*-quinone.

**Lewis Acidity (Scenarios A and C of Scheme 2).** If the Pd<sup>II</sup> complex was binding to the quinone in some fashion, we may be able to increase its binding ability by increasing its Lewis acidity. However, whereas *trans*-(Ph<sub>3</sub>P)<sub>2</sub>PdCl<sub>2</sub> is an excellent cocatalyst for the reaction, the presumably much more Lewis acidic (and harder, in hard–soft terminology) (Ph<sub>3</sub>P)<sub>2</sub>Pd(SbF<sub>6</sub>)<sub>2</sub> is ineffective; in fact, only trace amounts of the desired product were observed. Generally, when this occurs, one or two factors may be responsible: namely, the Lewis acid catalyzes ketene dimerization (such as Sc<sup>III</sup> does, eq 2), or the azaphilic Pd<sup>II</sup> complex quenches the nucleophilic cinchona alkaloid catalyst (also applicable to Sc<sup>III</sup>; see below). Additionally, *o*-chloranil's relative electron poverty would indicate that it is already fairly well activated and not as amenable to Lewis acid catalysis as the more electron-rich *o*-benzoquinone dimides.



**Potential Involvement of Palladium(0).** We must also account for whether Pd<sup>II</sup> or Pd<sup>0</sup>, possibly made in situ from a trialkylamine reductant or a contaminant of the commercially available *trans*-(Ph<sub>3</sub>P)<sub>2</sub>PdCl<sub>2</sub>, is the actual catalyst for the reaction. To perform this experiment, we reduced *trans*-(Ph<sub>3</sub>P)<sub>2</sub>PdCl<sub>2</sub> using LiAlH<sub>4</sub>.<sup>27</sup> This putative Pd<sup>0</sup> complex does not revert to Pd<sup>II</sup> upon reaction with the *o*-chloranil when stirred together cold or at 20 °C. We performed a test reaction using this Pd<sup>0</sup> cocatalyst and found the yield of the cycloaddition dropped from 55% for the metal-free reaction to 40%, indicating cocatalyst quenching by the Pd<sup>0</sup>. The same result was obtained when (PPh<sub>3</sub>)<sub>4</sub>Pd was used as the cocatalyst. Thus, Pd<sup>II</sup> must be the active form of the catalyst.

**Scenario B.** Together these experiments suggested that scenarios A and C (Scheme 2) do not occur (namely, the metal does not coordinate to *o*-chloranil), leaving scenario B to be further investigated and to establish ketene enolate formation. To determine the equilibrium ratio between ketene and ketene enolate, a low temperature UV–Vis experiment was performed with phenylethylketene (a more stable disubstituted ketene that does not readily dimerize), BQd, and *trans*-(Ph<sub>3</sub>P)<sub>2</sub>PdCl<sub>2</sub>, at a wavelength of 395 nm. Using a standard curve of phenylethylketene, the initial concentration of this reagent can be calculated and further monitored after addition of our Lewis base. In this experiment, when 1 equiv of BQd was added to the solution the ketene concentration decreased by 8.3%, the remainder resulting in ketene enolate formation (A, Figure 3). Quenching experiments with MeOH afforded a quantitative yield of the methyl 2-phenylbutanoate, as would be expected only if ketene and enolate were the only two species in equilibrium with each other. Once *trans*-(Ph<sub>3</sub>P)<sub>2</sub>PdCl<sub>2</sub> was added to the solution, another analogous shift in the equilibrium occurred,

(27) Kozitsyna, N. Y.; Moiseev, I. I. *Russ. Chem. Rev.* **1995**, *1*, 47–60.

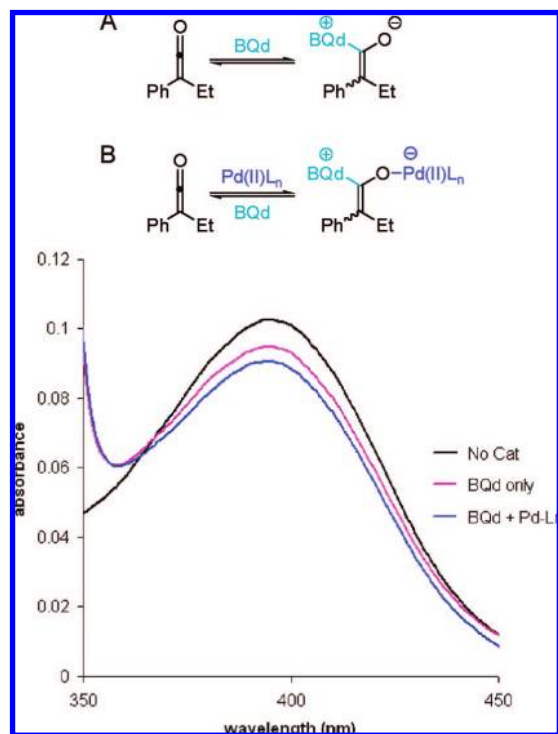


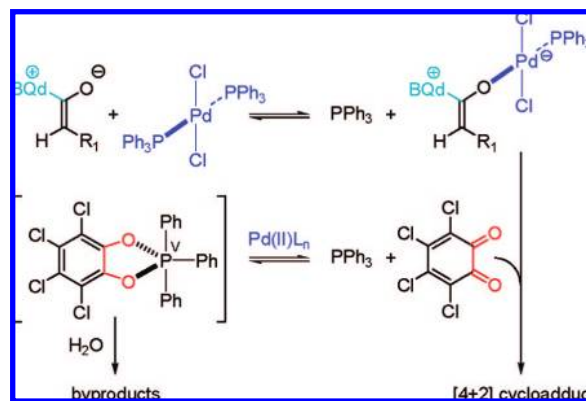
**Figure 3.** UV-vis profile of phenylethylketene showing the effects of BQd and *trans*-(Ph<sub>3</sub>P)<sub>2</sub>PdCl<sub>2</sub> on the ketene–enolate equilibrium.<sup>29</sup>

causing the ketene enolate concentration to increase to 11.5%. This corresponds to a 39% increase in ketene enolate concentration in the presence of the Pd<sup>II</sup> cocatalyst.<sup>28</sup> Once again, a methanol quench afforded the methyl ester quantitatively. These results suggest that a portion of the *trans*-(Ph<sub>3</sub>P)<sub>2</sub>PdCl<sub>2</sub> cocatalyst is coordinating to the ketene enolate (**B**, Figure 3) causing the overall enolate concentration to increase and suggest that the reaction proceeds through parallel metal-free and metal complexed manifolds (**B**, Scheme 2).

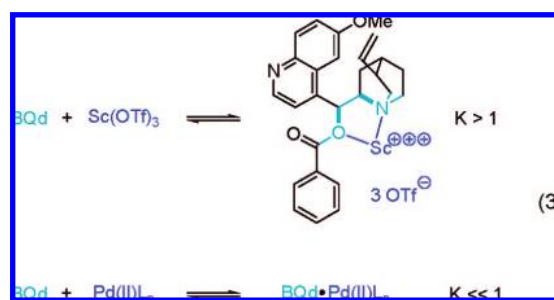
The data allow us to calculate equilibrium constants for the successive reactions that form metal-free ( $K = [\text{enolate } \mathbf{3a}]/[\text{ketene}][\text{BQd}] = 5.0 \times 10^{-2} \text{ M}^{-1}$ ) and metal-bound enolate ( $K = [\text{metal enolate } \mathbf{3b}][\text{PPh}_3]/[\text{enolate } \mathbf{3a}][\text{Pd complex}] = 1.6 \times 10^{-2}$ ). Solving for enolate concentrations indicates that, under normal reaction conditions, a substantial quantity of enolate could be metal-bound. As a caveat, the use of more stable and hindered disubstituted ketenes in the UV experiment provides a lower limit on the equilibria occurring under normal reaction conditions.

One question that arises is why Sc<sup>III</sup> does not bind observably to the enolate, as shown by our UV study. The answer may be that it is instead binding tightly to the catalyst. For example, a mixture of BQd and Sc(OTf)<sub>3</sub> reveals strong binding of the metal to the catalyst (eq 3), as shown by both IR spectroscopy and <sup>1</sup>H NMR  $\Delta\delta$ 's. For example, the carbonyl group frequency of BQd moves completely from 1728 to 1742 cm<sup>-1</sup> in the presence of 1 equiv of Sc(OTf)<sub>3</sub>, consistent with binding to the quinclidine N and the etheric ester O atoms. On the other hand, a similar experiment with (PPh<sub>3</sub>)<sub>2</sub>PdCl<sub>2</sub> shows no discernible binding; Pd<sup>II</sup> seems to be free to bind the enolate instead. These results also illustrate that it is dangerous to over-rely on simplified hard–soft acid–base theory. On this basis, one would

**Scheme 4.** Side Reaction of Ejected Triphenylphosphine



predict tighter binding of Sc<sup>III</sup> to the enolate, but in fact we observe the opposite, in part due to the presence of a competitive ligand.



**Formulating a Plausible Mechanistic Scenario.** The scenario that comes to mind is that the Pd<sup>II</sup> complex is involved in the formation of a metal enolate species. Transition metal based enolates have been postulated as intermediates in several asymmetric reactions;<sup>30</sup> in this case, the complex is presumably binding to either the oxygen or the carbon atom of the ketene enolate, stabilizing it and increasing its chemoselectivity toward quinone alkylation as opposed to nonproductive ketene dimerization. This could be one reason that several oxophilic metal salts do not work well in this reaction; they promote ketene dimerization or polymerization instead of the desired cycloaddition reaction. For instance, in the reaction with Sc(OTf)<sub>3</sub> cocatalyst, we noted a slower reaction (presumably due to cocatalyst binding shown in eq 3) and byproducts typical of oxophilic metal catalyzed reactions including ketene dimer and polymers. However, when the Pd<sup>II</sup> catalyst is combined with phenylethylketene at -78 °C in the absence of BQ, nothing happens—no ketene dimerization and no metal enolate.

In a parallel study, we conducted a control reaction in which 1 equiv of PPh<sub>3</sub> is mixed with *o*-chloranil in the presence of Pd<sup>II</sup>. NMR evidence is consistent with the formation of a P<sup>V</sup> intermediate<sup>31</sup> (Scheme 4) that decomposes to dihydrochloranil and triphenylphosphine oxide upon contact with water. However, this intermediate appears to form reversibly under the conditions of the control. Under our standard reaction conditions, phosphine-based byproducts are generally not observed.

**Density Functional Theory Calculations on Enolates.**<sup>25</sup> B3LYP/LANL2DZ calculations on Pd<sup>II</sup> complexes of ketene enolates

(28) This result was confirmed using two other stabilized ketenes.

(29) The UV spectrum is normalized at each end of the depicted region.

(30) Hamashima, Y.; Hotta, D.; Sodeoka, M. *J. Am. Chem. Soc.* **2002**, *124*, 11240–11241.

(31) Hellwinkel, D.; Wiel, A.; Sattler, G.; Nuber, B. *Angew. Chem.* **1990**, *102*, 677–680.

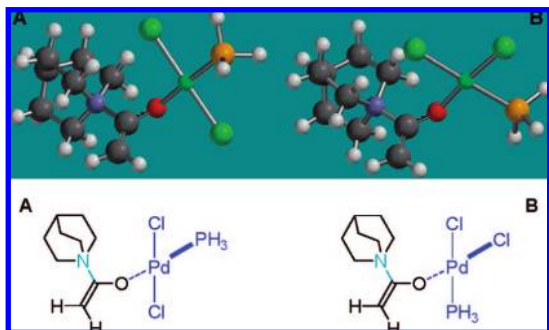


Figure 4. Optimized structures (LANL2DZ) of the Pd<sup>II</sup>–enolate complexes.

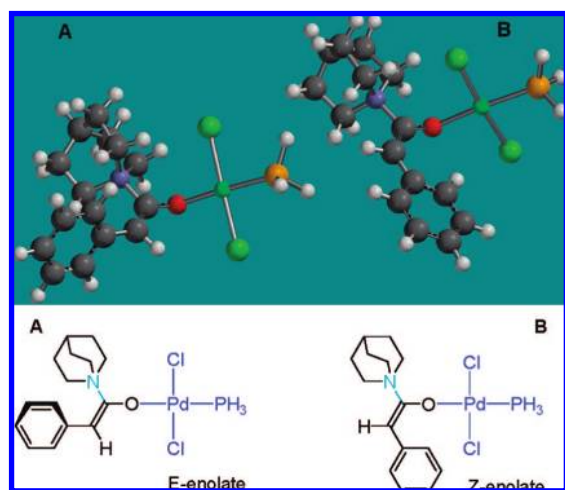


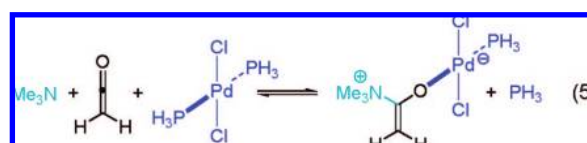
Figure 5. Calculations of the effect of palladium complexation on enolate isomerization.

show some interesting results. For example, during the calculation, Pd<sup>II</sup> exhibits a propensity to eject a phosphine ligand while binding fairly tightly to the ketene enolate oxygen. The Pd<sup>II</sup> generally optimizes to strict square-planarity (as one would expect from experimental literature precedent)<sup>32</sup> and has not shown any other geometric tendencies in calculations of this system (except octahedral coordination on occasion). On the other hand, binding of Pd<sup>II</sup> to the carbon atom of the enolate seems to be fairly high in energy comparatively. This prediction, combined with the obvious steric crowding of a carbon bound enolate, would seem to favor O-binding (a simplified model appears in Figure 4). The *trans*-substitution is calculated at lower total energy by 5.05 kcal/mol. The molecular orbital calculations indicate a substantial degree of charge on the nucleophilic terminal carbon (APT = −0.472); in contrast, the analogous quinuclidine–ketene–ScCl<sub>3</sub> complex is less highly charged at the terminus (APT = −0.442). According to these calculations, the Sc<sup>III</sup> fragment withdraws more electron density from the system, and the Pd<sup>II</sup> enolate presumably is more nucleophilic.

An interesting question involves why the metal cocatalyst exerts a small effect on the enantioselectivity. A clue may be provided by computations (B3LYP/LANL2DZ), which show that the *E/Z* ratio of the enolate is not much affected by the metal complex fragment and very much favors *Z* in all cases (B, Figure 5). We assume that a flip in enolate geometry could have a substantial impact on enantioselectivity. Even in employing the smaller quinuclidine as a model in the calculation, there was still an 8.14 kcal/mol stabilization for the *Z* enolate, relative to the *E*. What about the Pd<sup>II</sup> metal fragment affecting the facial

bias of the BQd catalyzed reaction rather than the *E/Z* ratio? It is quite possible that the sterically undemanding nature of the square-planar metal complex means that it simply does not get in the way; the Pd<sup>II</sup> cocatalyst has little or no effect on the enantioselectivity of the reaction.

On the other hand, the computed LANL2DZ energies of all species involved (enolates, metal catalyst, catalytic nucleophile, displaced phosphine) can give us a rough idea of the equilibrium constants for the formation of metal-free and metal-coordinated enolates (eqs 4 and 5). In this case, the approximate  $\Delta\Delta G$  in going to the metal-coordinated equilibrium (eq 5) is −7 kcal/mol (the fact that entropy changes for both equations are about the same<sup>33</sup> allowed us to correlate enthalpies to free energies). Thus, although we must view B3LYP energies at the LANL2DZ level with caution, qualitatively, it provides us with a rough guide to reaction energetics and suggests that the metal enolate species is the key to understanding catalysis in this system.



**Rate of Reaction Studies.** Initially, we observed that when we use Pd<sup>II</sup> as a cocatalyst, the reactions finished faster than the reactions that did not contain Pd<sup>II</sup>. While this does give us some information, the fact that in the presence of Pd<sup>II</sup> reactions finish in 1/2 to 1/4 the time does not necessarily mean that the palladium is involved in the rate-limiting step; it could simply increase the chemoselectivity of a step down the line. Previously, we have shown that the rate-limiting step of ketene enolate reactions is generally the dehydrohalogenation step,<sup>34</sup> so rate data that involve this RDS are then less interesting than could otherwise be. Most importantly, we found that the palladium does not affect the initial rate of acid chloride consumption.

Generally, our approach is to circumvent the uninteresting rate-limiting dehydrohalogenation by preformation of the ketene, which can be accomplished by a 2–6 h preliminary reaction of the acid chloride with NaH in the presence of catalysts BQd and 15-crown-5.<sup>34c</sup> When ketene formation is complete, we can then add the cocatalyst followed by the *o*-quinone; we then are assured of a more interesting rate-limiting step. Under these conditions, we found that Pd<sup>II</sup> increased the initial rate of reaction by 1.6-fold (Figure 6)<sup>35</sup>— a modest increase, but nevertheless surprising, implying that the monofunctional reaction is in fact operating in tandem with the bifunctional process. These concentration dependencies and the aforementioned UV equilibrium study allow us to formulate an overall rate equation for the reaction, which is segmented into monofunctional (BQd catalyzed) and bifunctional (BQd and Pd<sup>II</sup> catalyzed) components (eq 6).

$$\text{rate} = k[\text{ketene}][\text{BQd}][4] + k'[\text{ketene}][\text{BQd}][\text{trans}-(\text{Ph}_3\text{P})_2\text{PdCl}_2][4] \\ \text{rate} = k''[\text{metal-free enolate}][4] + k'''[\text{metal enolate}][4] \quad (6)$$

*monofunctional component*
*bifunctional component*

**Hartree–Fock Transition State Calculations.**<sup>25</sup> Another significant question is how the metal cocatalysts manage to increase



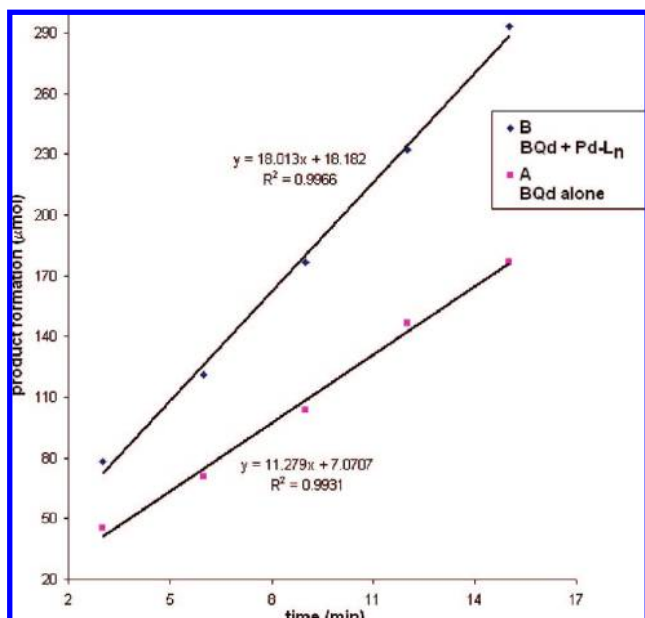


**Figure 6.** Initial plots of product formation vs time for monofunctional and bifunctional reactions: (A) BQd and *trans*-( $\text{Ph}_3\text{P}$ ) $_2\text{PdCl}_2$ ; (B) BQd.

the rate of reaction through enolate formation. Two main possibilities come to mind: (1) formation of a metal enolate lowers the activation barrier for carbon–oxygen bond formation; (2) the metal cocatalyst stabilizes the enolate, thus increasing its concentration and perhaps enhancing its chemoselectivity. We sought to address these questions through computations; in the first case, we compared transition states (TS) for C–O bond formation of the metal coordinated and metal free enolates. We examined streamlined model systems consisting of  $\text{Me}_3\text{N}$  as the catalytic nucleophile and ketene and *o*-chloranil as substrates (Figure 7).

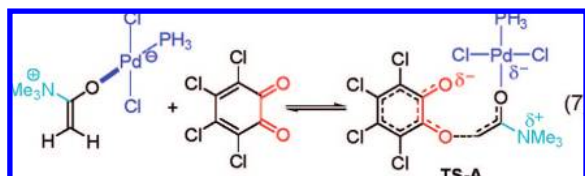
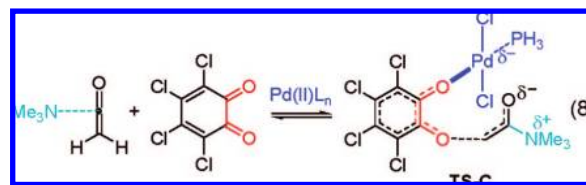


**Figure 7.** Calculated transition states for the reaction of *o*-chloranil with a model enolate in the presence (TS-A and TS-C) and absence (TS-B) of  $\text{Pd}^{\text{II}}$ .



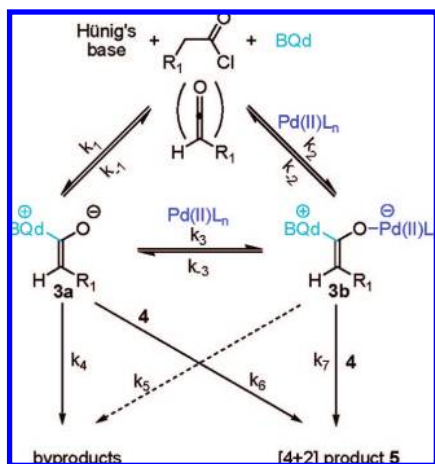
In the metal-coordinated cases (TS-A and TS-C), the fragment we employed was *trans*-( $\text{Ph}_3\text{P}$ ) $_2\text{PdCl}_2$ , which more or less mandates the use of the HF/3-21G\* basis set. In numerous attempts at a higher level of theory, the unconstrained geometry for TS-C did not converge. At HF/3-21G\*, the computed transition state for the attack of the metal bound enolate on *o*-chloranil (TS-A, eq 7) was 7.4 kcal/mol lower as compared to an isomeric transition state in which the metal binds to an *o*-chloranil oxygen (TS-C, eq 8). These relative energies should be fairly reliable as this level of theory goes; the gross atom connectivity in the two species is identical save for a migration of the metal from one oxygen to another. These results are in concert with experimental data supporting enolate activation, as opposed to *o*-chloranil activation—namely the perturbation in equilibrium observed in the UV study, and the lack of metal binding in the *o*-chloranil IR study.

**Palladium(II) Catalysis: A Summary.** We summarize several important factors which provide insight to the mechanism of palladium catalysis in this cycloaddition reaction: (1)  $\text{Pd}^{\text{II}}$  has no effect on the initial rate of acid chloride consumption, yet

(2) it increases the initial rate of product formation by 1.6-fold; (3)  $\text{Pd}^{\text{II}}$  suppresses byproduct formation and (4) increases the enolate concentration of a model system by 39%; (5)  $\text{Pd}^{\text{II}}$  does not observably coordinate to *o*-chloranil; (6) hard–soft Lewis acid–base considerations, especially the remarkable (almost total) difference in yield observed between *trans*-( $\text{Ph}_3\text{P}$ ) $_2\text{PdCl}_2$  and ( $\text{Ph}_3\text{P}$ ) $_2\text{Pd}(\text{SbF}_6)_2$  as cocatalysts; (7) the rate equation, which reveals concentration dependencies for *o*-chloranil, the ketene, BQd, and  $\text{Pd}^{\text{II}}$ . These all lead us to rationalize palladium's effect on the reaction in the following way (Scheme 5). The key to understanding this system lies in the chemoselectivity of the palladium enolate; we believe that  $k_7[\text{metal-bound enolate } \mathbf{3b}] > k_4[\text{metal-free enolate } \mathbf{3a}]$  and that  $k_5[\mathbf{3b}]$  is negligible. The modest overall rate increase of the reaction in the presence of the  $\text{Pd}^{\text{II}}$  complex is of secondary importance to the fact that  $\text{Pd}^{\text{II}}$  suppresses byproduct formation.

**Proposed Mechanism.** Analysis of the data allows us to formulate a mechanism for the *trans*-( $\text{Ph}_3\text{P}$ ) $_2\text{PdCl}_2$  cocatalyzed reaction (Scheme 6). The acid chloride, together with Hünig's base and BQd (**2a**), forms a chiral ketene enolate, which is in equilibrium with free ketene. Palladium then binds to the enolate, increasing its relative concentration and providing enhanced chemoselectivity toward the quinone. Once this cocatalyst-bound enolate and quinone react, they release both catalysts while forming the [4 + 2] cycloaddition product **5**.

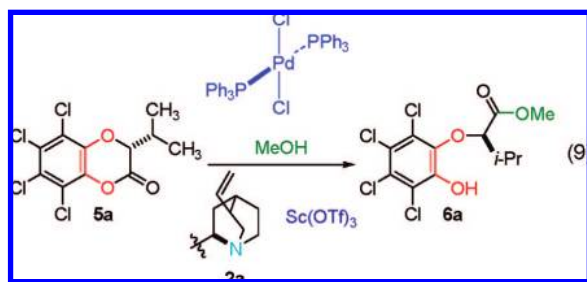


Scheme 5. Mechanistic Scenario to Explain Pd<sup>II</sup> Catalysis

To ensure that the palladium cocatalyst is indeed acting as a Lewis acid for a range of ketene enolates, a variety of acid chlorides were tested under the reaction conditions set forth above. We found a large increase in yield for each acid chloride tested, up to a 60% increase (Table 2).<sup>3</sup>

**Tandem Dioxinone Opening.** Ring opening of the initially formed bicyclic products **5** occurred smoothly under a variety of conditions. For example, the activated aryl lactones **5** react smoothly in situ with various nucleophiles, to produce  $\alpha$ -hydroxy acids, esters, amides, and thioesters, after oxidative workup, in high yields and excellent ee in most cases (Table 3). Slight racemization occurs with thiolysis (**7h**), whereas substantial erosion of ee occurs with ammonolysis (**7g**). Luckily, as shown below in the section on synthetic applications, the use of more complex amines for ring opening alleviates this problem.

**Promotion of Ring Opening Methanolysis.** When we began to use the palladium cocatalyst for the cycloaddition reaction (see Scheme 1), we noticed that the subsequent methanolysis reactions were faster in situ, obviating the need for an intermediate purification step. Upon further investigation, we found that both Pd<sup>II</sup> and BQd have a small but significant catalytic effect on the methanolysis of the cycloadduct and, when used together, they exhibit a larger effect by lowering reaction times significantly (eq 9).



In fact, when catalytic amounts (10 mol%) of *trans*-(Ph<sub>3</sub>P)<sub>2</sub>PdCl<sub>2</sub>, Sc(OTf)<sub>3</sub>, and BQd were added simultaneously to cycloadduct **5a**, the quantitative methanolysis proceeded faster than any combination of two of these catalysts, or any one alone, when the combined catalyst loading was kept at 10 mol% (see Figure 8 for various combinations). The initial rate of reaction was slightly over 3 times higher than that for uncatalyzed methanolysis. Although not a dramatic catalytic effect, this finding does represent a practical advance. As a standardized

procedure, the cycloaddition reaction is conducted in the presence of 10 mol% *trans*-(Ph<sub>3</sub>P)<sub>2</sub>PdCl<sub>2</sub> and BQd, which, upon completion, is followed by addition of a methanolic solution of 10 mol% Sc(OTf)<sub>3</sub>. We attempted to perform the cycloaddition reactions in the presence of all three catalysts, but this provided poor results, probably due to the aforementioned side reactions (ketene dimerization and BQd quenching) effected by Sc<sup>III</sup>. Mechanistically, one could postulate that BQd is acting as a catalytic nucleophile or base and that Sc<sup>III</sup> functions as a Lewis acid to activate the lactone carbonyl group. However, the way that Pd<sup>II</sup> augments the process remains somewhat mysterious, but it is clear that several reaction manifolds likely act in parallel.

**Applications.** A key feature of this methodology is its ability to access a variety of important classes of compounds in high yield and enantioselectivity, by simply modifying the acid chloride. As an example, by using 4-chlorobutryl chloride with BQ (**2b**),  $\gamma$ -lactam (*S*)-**11** can be made in 82% yield (4 steps) and >99% ee (Scheme 7). This intermediate is the key component in the synthesis of vasicinone, which serves as a remedy for bronchitis and asthma, and its formation here constitutes a formal total synthesis of (*S*)-(-)-vasicinone, the most efficient to date.<sup>36</sup>  $\gamma$ -Lactams are also known to be potent antibacterial agents,<sup>37</sup> HIV protease inhibitors,<sup>38</sup> and thrombin inhibitors.<sup>39</sup>

Analogously,  $\gamma$ -lactones have been employed as novel antibacterial and antitumor agents.<sup>40</sup> This structural unit frequently occurs in natural products including classes of alkaloids,<sup>41</sup> macrocyclic antibiotics,<sup>42</sup> and pheromones.<sup>43</sup> This valuable entity can be made by using 4-benzyloxybutyryl chloride to produce  $\gamma$ -lactone **10** in 88% yield (from *o*-chloranil) and >99% enantiomeric excess (Scheme 7).

Factor Xa is a serine protease within prothrombinase complexes that promotes blood coagulation through the conversion of prothrombin to thrombin. Selective inhibition of factor Xa has been demonstrated by compound **14**<sup>44</sup> and many analogous derivatives, the cores of which can be made by our asymmetric method (Scheme 8). The intermediate product resulting from a

- (32) Baber, R. A.; Orpen, A. G.; Pringle, P. G.; Wilkinson, M. J.; Wingad, R. L. *J. Chem. Soc., Dalton Trans.* **2005**, 659–667.
- (33) The change in the number of particles in going from starting materials to products is the same in both cases; this is generally believed to be an approximate “wash” in the amount of entropy.
- (34) (a) Taggi, A. E.; Hafez, A. M.; Wack, H.; Young, B.; Drury, W. J., III.; Lectka, T. *J. Am. Chem. Soc.* **2000**, *122*, 7831–7832. (b) Taggi, A. E.; Hafez, A. M.; Wack, H.; Young, B.; Ferraris, D.; Lectka, T. *J. Am. Chem. Soc.* **2002**, *124*, 6626–6635. (c) France, S.; Shah, M. H.; Weatherwax, A.; Wack, H.; Roth, J. P.; Lectka, T. *J. Am. Chem. Soc.* **2005**, *127*, 1206–1215.
- (35) For the first 18 min of the reaction, the relationship between product formation and time remains fairly linear.
- (36) Eguchi, S.; Suzuki, T.; Okawa, T.; Matsushita, Y.; Yashima, E.; Okamoto, Y. *J. Org. Chem.* **1996**, *61*, 7316–7319.
- (37) Kar, G. K.; Roy, B. C.; Das Adhikari, S.; Ray, J. K.; Brahma, N. K. *Bioorg. Med. Chem.* **1998**, *6*, 2397–2403.
- (38) Hungate, R. W.; Chen, J. L.; Starbuck, K. E.; Vacca, J. P.; McDaniel, S. L.; Levin, R. B.; Dorsey, B. D.; Guare, J. P.; Holloway, M. K.; Whitter, W. *Bioorg. Med. Chem.* **1994**, *2*, 859–879.
- (39) Okayama, T.; Seki, S.; Ito, H.; Takeshima, T.; Hagiwara, M.; Morikawa, T. *Chem. Pharm. Bull.* **1995**, *43*, 1683–1691.
- (40) Park, B. K.; Nakagawa, M.; Hirota, A.; Nakayama, M. *J. Antibiot.* **1988**, *41*, 751–758.
- (41) Schultz, A. G.; Shannon, P. J. *J. Org. Chem.* **1985**, *50*, 4421–4425.
- (42) Hein, M. S.; Gloer, J. B.; Koster, B.; Malloch, D. *J. Nat. Prod.* **2001**, *64*, 809–812.
- (43) Dos Santos, A. A.; Francke, W. *Tetrahedron: Asymmetry* **2006**, *17*, 2487–2490.
- (44) Su, T.; Zhu, B.-Y.; Kane-Maguire, K.; Scarborough, R. M.; Zhang, P. *PCT Int. Appl.* **2000**, 2000071510.

Scheme 6. Proposed Bifunctional Mechanism for the Palladium(II) Cocatalyzed Reaction

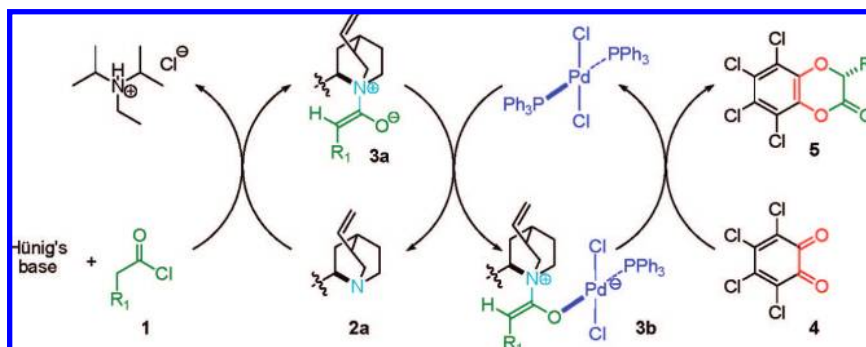
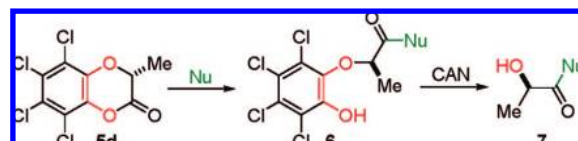


Table 2. Effects of Palladium Cocatalyzed Reaction on Product Yield

entry	Structure	no metal		10 mol% $trans\text{-}(PPh_3)_2PdCl_2$	
		% ee	% yield	% ee	% yield
1		93	55	93	88
2		99	63	99	81
3		99	49	98	77
4		96	59	96	86
5		93	64	94	87

Table 3. Nucleophilic Opening of 1,4-Benzodioxinones



entry <sup>a</sup>	Nu	% ee	% yield <sup>d</sup>
1	7d, MeOH <sup>b</sup>	96	88
2	7f, H <sub>2</sub> O <sup>b</sup>	97	87
3	7g, NH <sub>4</sub> OH <sup>c</sup>	80	82
4	7h, PhSH <sup>c</sup>	92	80

<sup>a</sup> Cycloaddition reactions run under standard conditions, quenched with nucleophile, then warmed to room temp. <sup>b</sup> 3 mL. <sup>c</sup> 1 equiv. <sup>d</sup> Isolated yield for three steps from *o*-chloranil, 4.

cycloaddition of **12** with phenylacetylchloride under standard bifunctional conditions is opened up in situ by aniline **13** to yield the inhibitor **14** in 93% overall yield and >99% ee.

In a final and very successful case, *N*-[*N*-(3,5-difluorophenylacetyl)-*L*-alanyl]-(*S*)-phenylglycine *tert*-butyl ester (DAPT) and its derivatives are known to be potent inhibitors of  $\beta$ - and  $\gamma$ -secretases that have been linked to Alzheimer's disease.<sup>45</sup> For example, hydroxy DAPT derivative **17** has been shown as a potent BACE-1 inhibitor, which initiates the production of amyloidogenic  $A\beta$  peptide, the principle component in plaque in AD patients.<sup>45</sup> Our catalytic, asymmetric method allows the facile production of the chiral  $\alpha$ -hydroxyl group which is responsible for a 10-fold increase in activity for **17** versus DAPT (Scheme 9).

Cycloaddition of 3,5-(difluoro)phenylacetyl chloride and *o*-chloranil under standard conditions yields intermediate "active-ester" cycloadduct **15**. On the other hand, a standard peptide coupling yields precursor **16** in 94% yield; in situ addition of **16** to the crude reaction mixture effects ring-opening acylation of the active-ester **15**. The major product was immediately subjected to CAN oxidation to form the final product **17** in high overall yield (87% from *o*-chloranil) and >99% ee.

## Conclusion

We have documented a novel asymmetric, bifunctional hetero-Diels–Alder reaction to afford useful  $\alpha$ -oxygenated products in excellent yield and enantioselectivity. By undertaking mechanistic studies based on the integration of experimental and calculated data, we demonstrated a surprising cooperative LA/LB interaction on a ketene enolate, rather than classical LA activation of the heterodiene and LB activation of the ketene enolate dienophile, as we had seen before in two other [4 + 2] inverse-electron-demand hetero-Diels–Alder reactions. By exploiting this mechanistic "switch," we have optimized our method for the synthesis of highly enantiomerically enriched  $\alpha$ -hydroxy acids, esters, amides, thioesters, lactones, and lactams and have demonstrated applications to timely biological targets. In summary, this is a rare example of a substrate that is activated by a Lewis acid and a Lewis base in a tandem fashion to form

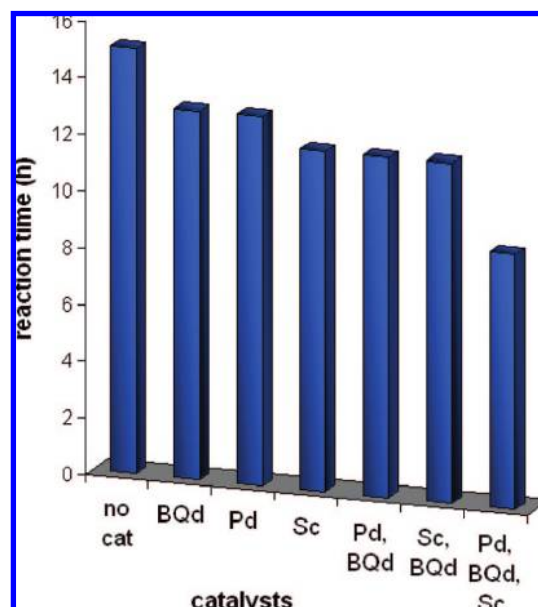
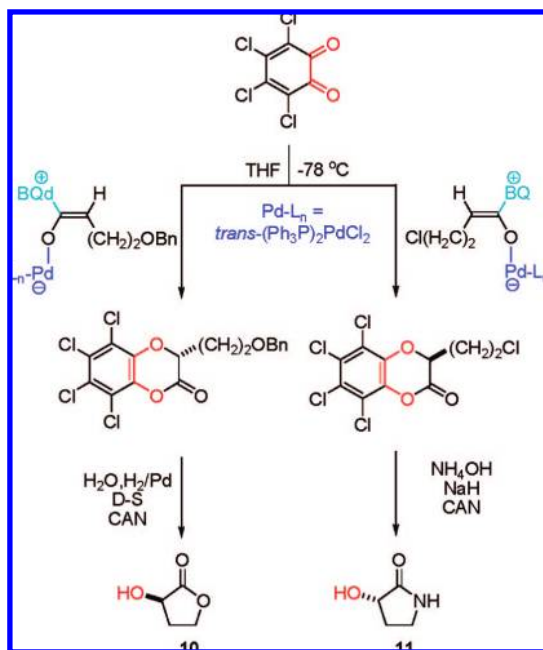
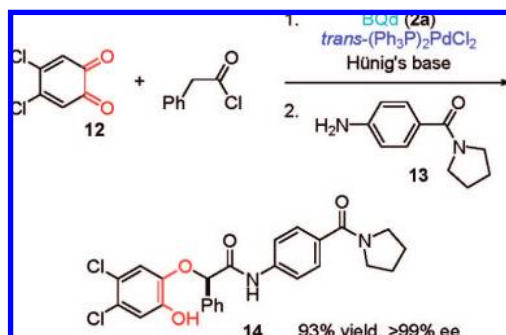
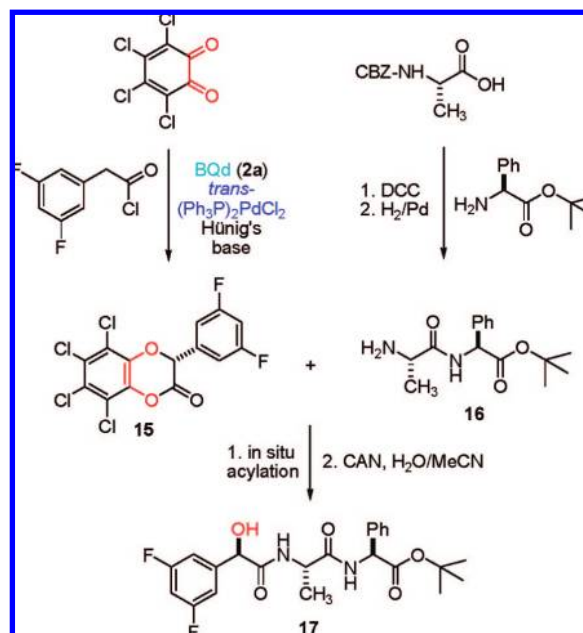


Figure 8. Comparative reaction times of catalytic methanolysis of cycloadduct **5a** in the presence of various promoters.

**Scheme 7.** Synthesis of  $\alpha$ -Hydroxy- $\gamma$ -lactone **10** and  $\alpha$ -Hydroxy- $\gamma$ -lactam **11****Scheme 8.** Synthesis of the Factor Xa Inhibitor

$\alpha$ -oxygenated products. This method, along with its unusual mechanistic features, compares highly favorably to other syntheses of these desirable and useful chiral building blocks.

**Scheme 9.** Synthesis of  $\alpha$ -Hydroxyl DAPT

**Acknowledgment.** T.L. thanks the NIH (GM064559) for support. T.B. thanks the NIH as well for a Minority Supplement Fellowship, D.H.P. thanks Johns Hopkins for a Zeltmann Fellowship, and T.D. would like to thank NSERC, CFI, and Merck. The authors also thank Branden Fonovic for his help with the DFT calculations and Professor Kenneth Karlin for the use of his UV spectrometer.

**Supporting Information Available:** General procedures for the synthesis  $\alpha$ -hydroxyesters and  $\alpha$ -hydroxyamides, compound characterization, and complete information on the DFT calculations are provided, as well as complete refs 4, 6, and 7. This material is available free of charge via the Internet at <http://pubs.acs.org>.

JA806818A

(45) Pietrancosta, N.; Quelever, G.; Laras, Y.; Garino, C.; Burlet, S.; Kraus, J. L. *Aust. J. Chem.* **2005**, *58*, 585–594.